Microvoid formation in low-temperature molecular-beam-epitaxy-grown silicon

D. D. Perovic* and G. C. Weatherly†
Department of Metallurgy and Materials Science, University of Toronto, Toronto, Canada M5S 1A4

P. J. Simpson and P. J. Schultz
Department of Physics, The University of Western Ontario, London, Canada N6A 3K7

T. E. Jackman, G. C. Aers, J.-P. Noël, and D. C. Houghton
Institute for Microstructural Sciences, National Research Council, Ottawa, Canada K1A 0R6
(Received 25 February 1991)

In a study of (100) Si growth by molecular-beam epitaxy, we have observed an interesting growth phenomenon associated with epitaxial growth at low temperatures. Electron-microscope imaging reveals that the growth surface no longer remains planar but develops a series of cusps with {111}-oriented facets that generate linear arrays of spherical defects. Both electron microscopy and variable-energy positron-annihilation spectroscopy have been used to determine that the defects are in fact microvoids.

INTRODUCTION

In the fabrication of Si-based structures by molecular-beam epitaxy (MBE), the general trend toward the use of lower growth temperatures has resulted in the improvement of coevaporative doping control and the realization of highly metastable, elastically strained heterostructures. Accordingly, it is of fundamental interest to understand fully the structural limitations of low-temperature Si-MBE growth.

Jorke *et al.*[1,2] studied the breakdown of epitaxial growth at low temperatures as a function of Si deposition rate for both constant and variable temperature growths. They observed the transition from single crystalline to polycrystalline (twinned) and finally amorphous growth. A transition rate equation was used to model their data which successfully predicted the breakdown of epitaxy beyond a certain critical thickness at constant temperature and deposition rate.[2] More recently, Eaglesham, Gossman, and Cerullo[3] confirmed the existence of a limiting epitaxial thickness that exhibited an exponential temperature dependence as theoretically predicted by Jorke *et al.*[2] However, Eaglesham, Gossman, and Cerullo[3] did not observe the intermediate polycrystalline transition as the single crystal transformed to the amorphous state. Interestingly, Liliental-Weber[4] has also observed a polycrystalline transition at the critical thickness for epitaxial growth of GaAs at 200 °C. In this Brief Report we report for the first time on the generation of microvoid regions within low-temperature epitaxial Si which are formed prior to the breakdown of epitaxy via polycrystalline-amorphous transformations.

The Si layers of this study were grown in a VG Semicon V80 MBE system on (100) Czochralski Si substrates rotated at 30 rpm. The substrate surface prior to growth was cleaned *in situ* by heating to > 850 °C under a 0.01-nm/s Si flux to remove a sacrificial oxide.[5] The substrate temperature was calibrated above 350 °C with an optical pyrometer (bandwidth, 0.9–1.08 μm); lower growth temperatures were estimated from an extrapolation of this calibration. We have examined several samples grown both at constant temperature and with a decreasing temperature ramp.

Samples were studied using a number of transmission electron microscopy (TEM) techniques in cross-sectional and plan-view geometries; thin foils were prepared in the standard way using argon atom milling. Parallel to the microscopy study, a complementary investigation using variable-energy positrons was used to identify and depth profile the defects in bulk samples.

ELECTRON MICROSCOPY

Figure 1(a) is a weak beam image of one of one of a number of thick (6.3 μm) p-n-n^+ structures grown at constant temperature (400 °C) in a relatively poor vacuum (5×10^{-8} Torr) at a growth rate of 0.5 nm/s. There are several contrast features to note in the microstructure. First, the substrate-epilayer interface is clearly resolved because of the incomplete removal of oxygen and/or carbon from the wafer surface prior to growth. It can be seen that a high density of threading dislocations and stacking faults has been generated at interfacial precipitates.[5] Examination of the regions between the dislocations revealed a peculiar contrast effect which initiates ~0.6 μm beyond the substrate-epitaxial layer interface *independent* of dislocation and stacking fault generation and continues to the wafer surface.[6] This is clearly resolved at higher magnifications, as in Fig. 1(b), which reveal linear arrays of spherical defects images (3–6 nm in diameter) aligned parallel to the [100] growth direction. The defects are visible with high-diffraction contrast because the two-beam extinction distance ξ_g within the defect regions is much larger relative to the Si matrix as manifest by the transition from white to black across a given thickness fringe; such large shifts in ξ_g are consistent with either amorphous or void regions in crystals.[7]

Closer to the free surface of the wafer [Fig. 1(c)], the spherically shaped defects were found to evolve from

morphologically unstable, cylindrically shaped regions which in turn originated at the base of cusps at the free surface. From direct lattice imaging of [011]-oriented cross sections it was determined that the cusps are faceted along {111} traces. It should be emphasized that the defect structures were visible solely by structure factor contrast as no strain contrast was observed under any diffracting condition. Furthermore, from plan-view images of thin foils with [100] surface normals, it was clear that the arrays of defects adopt a very regular arrangement with a well-defined average spacing.

The heterostructure shown in Fig. 2 was grown at a lower temperature (300 °C) and growth rate (0.1 nm/s) under typical vacuum conditions (1×10^{-9} Torr). Furthermore, the original substrate-heterostructure interface was featureless on the scale of cross-sectional TEM, indicative of excellent surface preparation prior to growth. The Ge-Si/Si strained-layer superlattice (SLS) possesses perfect interfaces except where threading dislocation segments are seen to nucleate. At a greater thickness (denoted by arrows), the generation of spherical [100]-oriented defect arrays is again observed in the epitaxial Si. As the epitaxial layer thickness increases, the {111}-oriented cusps become larger and eventually impinge wherein microtwins and stacking faults can nucleate during the first stages of the polycrystalline transformation (epitaxy breakdown). It is particularly interesting to note that the linear defect arrays generated within the epitaxial region extend through the polycrystalline region into the amorphous material where a similar contrast feature is observed.

A fully dynamical contrast analysis was carried out from two-beam images as shown in Fig. 1(b). Based on the foil thickness dependence of the defect images in bright and dark field, it was determined using existing theory[8] that the defects behave as voids located at various depths within the thin foil. Consistent results were also obtained from multibeam lattice images of the spherically shaped defect regions [see Fig. 1(b)] since the phase contrast showed a strong defect depth dependence within the foil at constant thickness. Depth-dependent contrast effects of this type have been observed previously by Howie and Hutchison[9] for small voids present in platelet defects in diamond as predicted by Bloch-wave scattering theory. In a later series of experiments we attempted to resolve the defect structure directly using scanning transmission electron microscopy (STEM). The three-dimensional nature of STEM imaging clearly indicated

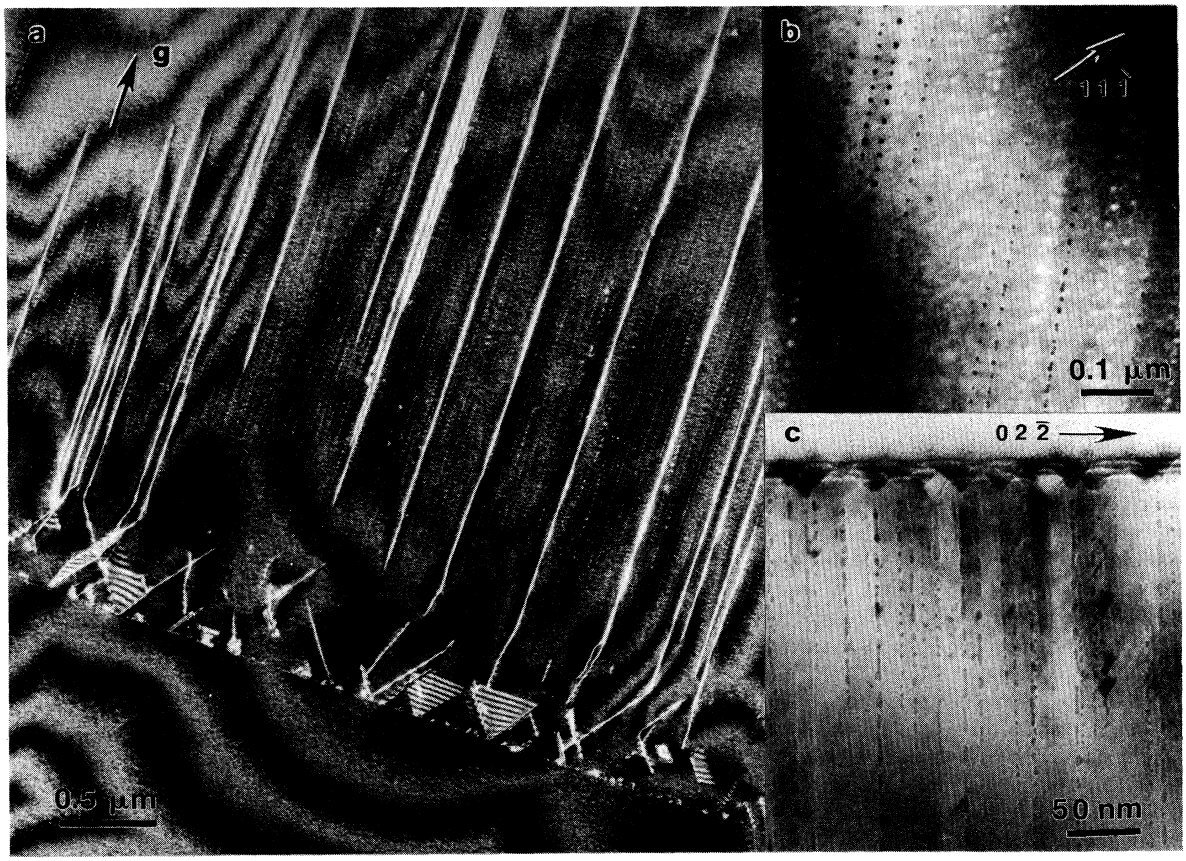

FIG. 1. (a) Weak-beam image [$\mathbf{g}=(800)$] of a homoepitaxial Si layer grown at 400 °C viewed in [011] cross section. Dislocations and stacking faults are generated at carbon and/or oxygen precipitates retained at the original substrate surface. (b) Higher-magnification dark-field image [$\mathbf{g}=(11\bar{1})$] showing spherical microvoids surrounded by epitaxial Si. (c) Bright-field image [$\mathbf{g}=(02\bar{2})$] showing the nonplanar surface of the epitaxial layer and the formation of cylindrical-spherical microvoid regions.

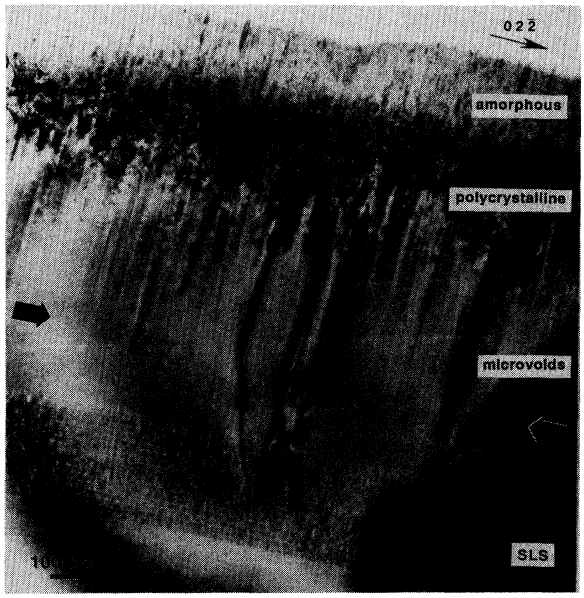

FIG. 2. Cross-sectional bright-field image [$\mathbf{g}=(02\bar{2})$] of a Ge_xSi_{1-x}/Si heterostructure grown at 300 °C. Microvoids are generated within the epitaxial Si region which subsequently breaks down via a polycrystalline-amorphous transformation; the linear array of microvoids persists through to the amorphous material.

that the surface is replete with voids since the foil was thinned from the substrate side; the diameter of the microvoid regions was similar to the width of the cusps at the free surface as seen in Fig. 1(c). A similar conclusion was obtained from large-tilt scanning electron microscope (SEM) images of the bulk wafer surface which clearly resolved the microvoid structure. Finally, and perhaps most importantly, upon annealing samples to a temperature above which solid-phase epitaxial regrowth of amorphous Si should have occurred (30 s at 700 °C), the defect structures were not removed but instead showed faceting of their internal surfaces along {111} traces.

POSITRON ANNIHILATION SPECTROSCOPY

After the first observation of the spherical defects, and knowing that the interpretation of structural images from specimens requiring sample preparation for electron microscopy can be nonrepresentative of the bulk, we initiated a parallel study on bulk material using variable-energy positron-annihilation spectroscopy in order to unambiguously identify the defect type. The use of positron annihilation to determine the type of point defects and their depth distribution in the near-surface region of solids has been reviewed recently.[10] Briefly, a beam of monoenergetic positrons is implanted into the sample where the positron loses its energy (thermalization) and then diffuses through the solid until annihilating either from this freely diffusing state or from a trapped state (bulk defect or a surface state). By changing the implantation energy (tunable 0–60 keV), different depths of the sample can be probed. The annihilation radiation (511-keV γ rays) is Doppler broadened due to the finite momentum of the annihilation pair (i.e., electron). The sensitivity arises from the different electronic environments of the defects which in turn produce a change in the measured γ-ray energy distribution. This distribution is normally characterized by one of a number of different shape parameters; in this case we have used the W parameter[10] which is the ratio of counts in the "tails" of the annihilation spectrum to the total counts.[11] The measurements were made using the University of Western Ontario Slow-Positron-Beam facility which has been described in detail elsewhere.[12]

Figure 3 shows the W parameter measured as a function of positron implant energy E for a defect-free Si(100) crystal as shown by open triangles. For very low implant energies, annihilations occur in the surface oxide layer ($W_s \sim 0.29$) whereas for very high energies, essentially all annihilations occur in the freely diffusing state ($W_f \sim 0.24$). A smooth transition between these values as observed as the energy increases. Also shown, by crosses, are data from the same crystal after amorphization by 1-MeV Pt ions. In the defected region, the positrons become trapped and annihilate with $W_d \approx 0.93 W_f$. Other defect values that have been reported for silicon to date range from $W_d/W_f \sim 0.93$ to ~ 1.10 for monovacancies or divacancies, impurity-vacancy or interstitial complexes.[13–16]

The W versus E curve for the sample depicted in Fig. 1 is shown in Fig. 3 by open circles. Immediately apparent is the exceptionally large decrease in the W parameter compared to the amorphized sample or any other reported point defect complex. The extremely narrow line-shape parameter observed ($W_d/W_f \ll 0.93$) is clear evidence that the spherical defects are microvoids and not regions of amorphous Si. The narrow line shape can be

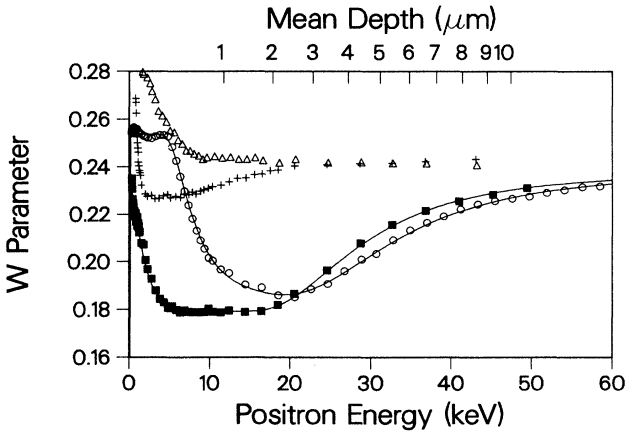

FIG. 3. Doppler-broadened annihilation line-shape parameter W as a function of incident positron energy or mean implant depth. The curves are as follows: Czochralski-grown Si(100) wafer (△), Czochralski-grown Si(100) wafer after amorphization by 1-MeV Pt ion implantation (+), Si epilayer shown in Fig. 1 including B_2O_3 capping layer (○), and Si epilayer shown in Fig. 1 after chemical etching of top 1.2 μm (■).

due only to the very low center-of-mass momentum of either positronium formation inside a void or, alternatively, trapping into positroniumlike states on the inner surface of a void.[10,11]

The flat region at low energy (~ 0.255) occurs because of saturation trapping at oxygen-related defects in the p^+-type (B_2O_3 doped[17]) capping layer and clearly illustrates the capability of the technique to profile different defect types. Removal of this layer (1.2 μm) by chemical etching and remeasurement (solid squares in Fig. 3) accentuated the extremely low value of W without the dilution of the oxygen-related annihilations. The curves shown are fits to the data using the program POSTRAP4[18] and the same defect parameters for both curves (within 2%).

DISCUSSION

Several Si-based structures, both homoepitaxial and heteroepitaxial, with and without doping, have been grown under different conditions yet reproducibly exhibit microvoid formation. Although the development of a regular array of rods or spheres aligned in the growth direction is a characteristic feature of a monotectic or eutectic transformation in two-phase alloys, we believe this is the first observation of an aligned void structure in a single-crystalline-phase material under any growth conditions. The evolution of the microvoid structure is clearly associated with the faceting of the growth surface; the (100) surface breaks down into a series of cusps and peaks, each cusp having a pyramidal structure bounded by {111} facets. The development of the cusps precedes the formation of voids, but on continued growth, cylindrical voids are left in the wake of the migrating surface at each cusp. These cylindrical channels become morphologically unstable, the classic Rayleigh instability, and break up to form a series of aligned voids. In the absence of any neighboring vacancy sinks, the voids facet on {111} on annealing, but are otherwise stable.

It is interesting to speculate what role, if any, the development of a faceted growth surface and its associated void structure plays in the crystalline-amorphous transition discussed in the recent papers of Jorke *et al.*[1,2] and Eaglesham, Gossman, and Cerullo.[3] We have found that where a "regular," albeit faceted, growth front develops, growth can proceed to thicknesses well in excess of those predicted by Jorke *et al.*[2] and observed by Eaglesham, Gossman, and Cerullo[3] without epitaxy breakdown. The results of Fig. 1 show a 6.3-μm-thick Si layer grown at 400 °C where "perfect" epitaxy occurred for 0.6 μm followed by a well-developed void–single-crystal structure visible for approximately 6 μm. Similarly, in the sample grown at 300 °C (see Fig. 2), we observe perfect epitaxy for 1.8 μm followed by 0.5 μm of microvoid Si prior to epitaxy breakdown. We have never observed the abrupt perfect single-crystal–amorphous transition reported by Eaglesham, Gossman, and Cerullo.[3] When epitaxy breaks down, it does so by the formation of a well-defined polycrystalline layer associated with the development of a high microtwin and stacking fault density at the {111} cusps. On continued growth these areas lead to the "conelike" features described by Jorke *et al.*[1,2] which we observe for both constant and ramped temperature growths. At this point there is no simple explanation that can account for these differences between our study and that of Eaglesham, Gossman, and Cerullo.

*Present address: Cavendish Laboratory, Department of Physics, University of Cambridge, Madingley Road, Cambridge CB3 0HE England.

†Present address: Department of Materials Science and Engineering, McMaster University, Hamilton, Canada L8S 4L7.

[1]H. Jorke, H.-J. Herzog, and H. Kibbel, Phys. Rev. B **40**, 2005 (1989).

[2]H. Jorke, H. Kibbel, F. Schäffler and H.-J. Herzog, Thin Solid Films, **183**, 307 (1989).

[3]D. J. Eaglesham, H.-J. Gossman and M. Cerullo, Phys. Rev. Lett. **65**, 1227 (1990).

[4]Z. Liliental-Weber, in *Epitaxial Heterostructures,* edited by D. W. Shaw, J. C. Bean, V. G. Keramidas, and P. S. Peercy, MRS Symposia Proceedings No. 198 (Materials Research Society, Pittsburgh, 1990), p. 371.

[5]D. D. Perovic, G. C. Weatherly, J.-M. Baribeau, and D. C. Houghton, Thin Solid Films **183**, 141 (1989).

[6]The same substrate-induced stacking faults and dislocation segments were observed in an identical structure grown at 750 °C under similar vacuum conditions. However, the linear defect features were not present in the microstructure.

[7]M. F. Ashby and L. M. Brown, Philos. Mag. **8**, 1649 (1963).

[8]J. van Landuyt, R. Gevers, and S. Amelinckx, Phys. Status Solidi **10**, 319 (1965).

[9]A. Howie and J. L. Hutchison, J. Microsc. **142**, 131 (1986).

[10]P. J. Schultz and K. G. Lynn, Rev. Mod. Phys. **60**, 701 (1988).

[11]The spectrometer settings were as follows: tail regions (507.34→509.73 keV+512.27→514.66 keV) divided by the total region (506.22→515.78 keV).

[12]P. J. Schultz, Nucl. Instrum. Methods B **30**, 94 (1988).

[13]S. Dannefaer and D. Kerr, J. Appl. Phys. **60**, 1313 (1986).

[14]J. Keinonen, M. Hautala, E. Rauhala, V. Karttunen, A. Kuronen, J. Räisänen, J. Lahtinen, A. Vehanan, E. Punkka, and P. Hautojärvi, Phys. Rev. B **37**, 8269 (1988).

[15]P. J. Schultz, E. Tandberg, K. G. Lynn, B. Nielsen, T. E. Jackman, M. W. Denhoff, and G. C. Aers, Phys. Rev. Lett. **61**, 187 (1988).

[16]T. E. Jackman, G. C. Aers, M. W. Denhoff, and P. J. Schultz, Appl. Phys. A **49**, 335 (1989).

[17]T. E. Jackman, D. C. Houghton, J. A. Jackman, M. W. Denhoff, S. Kechang, J. McCaffrey, and A. Rockett, J. Appl. Phys. **66**, 1984 (1989).

[18]G. C. Aers, in *Positron Beams for Solids and Surfaces,* edited by P. J. Schultz, G. Massoumi, and P. J. Simpson (AIP, New York, 1990).

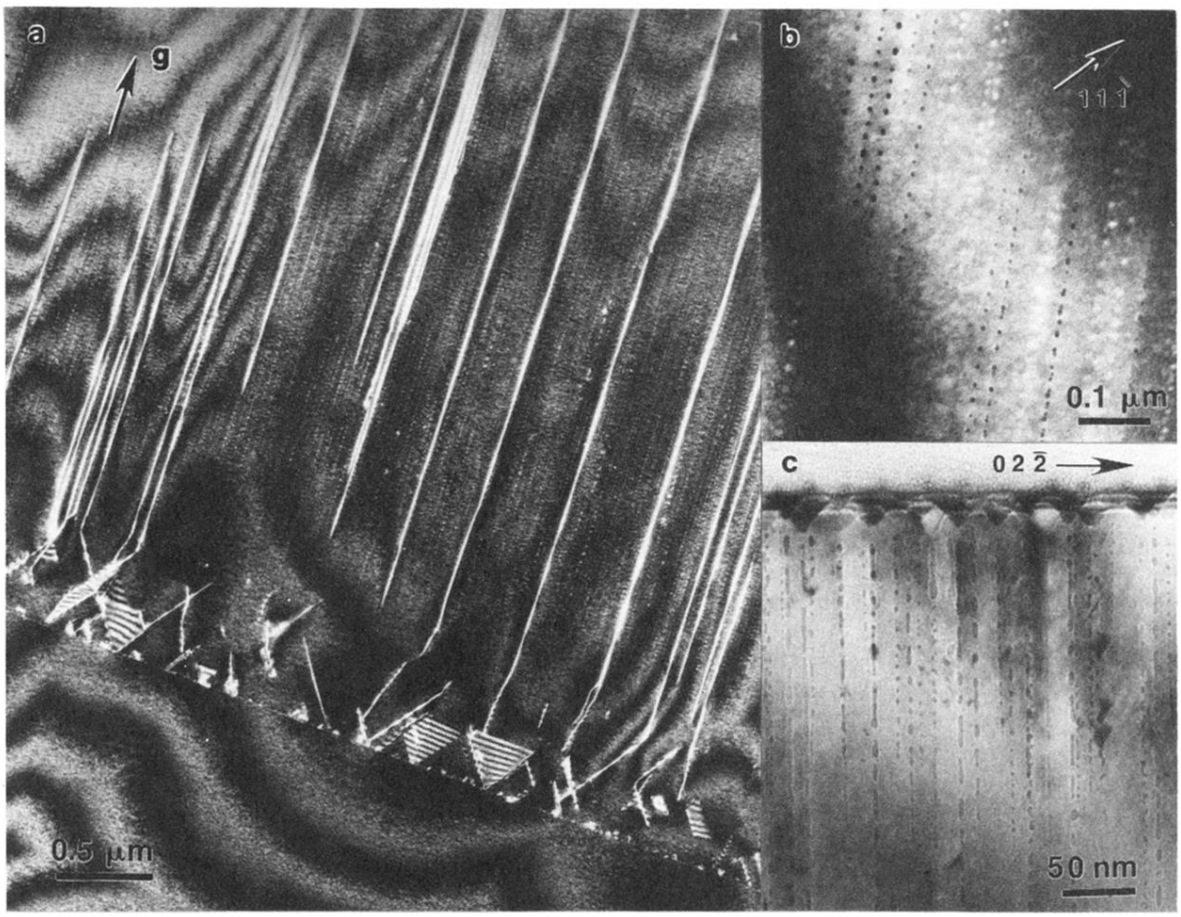

FIG. 1. (a) Weak-beam image [$\mathbf{g}=(800)$] of a homoepitaxial Si layer grown at 400 °C viewed in [011] cross section. Dislocations and stacking faults are generated at carbon and/or oxygen precipitates retained at the original substrate surface. (b) Higher-magnification dark-field image [$\mathbf{g}=(11\bar{1})$] showing spherical microvoids surrounded by epitaxial Si. (c) Bright-field image [$\mathbf{g}=(02\bar{2})$] showing the nonplanar surface of the epitaxial layer and the formation of cylindrical-spherical microvoid regions.

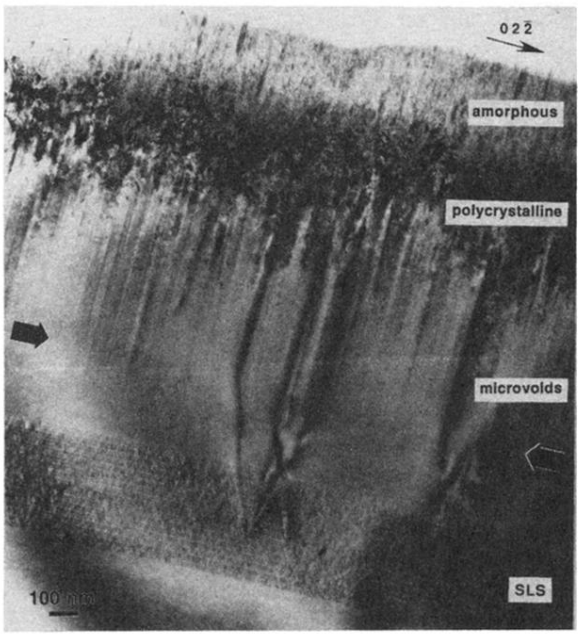

FIG. 2. Cross-sectional bright-field image [$\mathbf{g}=(02\bar{2})$] of a Ge_xSi_{1-x}/Si heterostructure grown at 300 °C. Microvoids are generated within the epitaxial Si region which subsequently breaks down via a polycrystalline-amorphous transformation; the linear array of microvoids persists through to the amorphous material.